***International Journal of Minerals, Metallurgy and Materials***
***Volume 30, Number 4, April 2023, Page 782***
**https://doi.org/10.1007/s12613-022-2502-8**

# Eco-friendly physical blowing agent mass loss of bio-based polyurethane rigid foam materials

*Haozhen Wang, Lin Lin, and Yingshu Liu*✉

School of Energy and Environmental Engineering, University of Science and Technology Beijing, Beijing 100083, China

(Received: 19 January 2022; revised: 15 April 2022; accepted: 15 April 2022)

**Abstract:** Through systematical experiment design, the physical blowing agent (PBA) mass loss of bio-based polyurethane rigid foam (PURF) in the foaming process was measured and calculated in this study, and different eco-friendly PBA mass losses were measured quantitatively for the first time. The core of the proposed method is to add water to replace the difference, and this method has a high fault tolerance rate for different foaming forms of foams. The method was proved to be stable and reliable through the standard deviations $\sigma_1$ and $\sigma_2$ for $R_1$ (ratio of the PBA mass loss to the material total mass except the PBA) and $R_2$ (ratio of the PBA mass loss to the PBA mass in the material total mass) in parallel experiments. It can be used to measure and calculate the actual PBA mass loss in the foaming process of both bio-based and petroleum-based PURF. The results show that the PBA mass loss in PURF with different PBA systems is controlled by its initial mass content of PBA in PU materials $\omega$. The main way for PBA to dissipate into the air is evaporation/escape along the upper surface of foam. This study further reveals the mechanism of PBA mass loss: the evaporation/escape of PBA along the upper surface of foam is a typical diffusion behavior. Its spread power comes from the difference between the chemical potential of PBA in the interface layer and that in the outside air. For a certain PURF system, $R_1$ has approximately linear relationship with the initial mass content of PBA in PU materials $\omega$, which can be expressed by the functional relationship $R_1 = k\omega$, where $k$ is a variable related to PBA's own attributes.

**Keywords:** polyurethane; bio-based polyol; eco-friendly physical blowing agent; mass loss

## 1. Introduction

Polyurethane (PU) play a significant role in global industry with over three-quarters of the consumption in the form of foams [1]. Blowing agent (BA) is needed in the production of polyurethane rigid foam (PURF), among which physical blowing agent (PBA) has the largest amount. PBA usually is low boiling point liquids, and when PBA is heated above its boiling point, it evaporates through physical phase transition to play the role of foaming [2–3]. HCFC-141b, HFC-245fa, and HFC-365mfc currently are the most widely used PBAs in the PU foam industry [1]. They are relatively more eco-friendly than CFC-11 [4]. The fully eco-friendly PBAs, such as HFCO-1233zd(E) and HFO-1336mzz(Z) [5], which have 0 ODP (ozone depletion potential) and low GWP (global warming potential), play an important role in PU foam industry. For each generation of PBA system, the relevant properties are described in Table 1.

PURF needs to go through a complex process from a low viscosity liquid to a high viscosity gel, and finally to a solid. In this process, there will be a certain amount of PBA mass loss. The mass loss of flammable PBA has a significant impact on production safety and environmental pollution. The price of non-flammable eco-friendly PBA is higher, and its mass loss will increase the product cost. Accurate measurement of PBA mass loss in foaming process can provide reasonable control basis for production safety; it can provide effective data for environmental protection equipment setting and parameter matching. We can also analyze the proportion of PBA with the lowest loss rate and the best economy.

Due to the complexity of PURF foaming process, which is accompanied by mass transfer, heat transfer, gasification, escape, condensation, and other processes, the measurement of dynamic PBA mass loss is extremely difficult in the foaming process, and at the same time, it is easy to cause the result distortion due to too many variables. Baser and Khakhar [6–7], when studying the kinetics simulation of PBA foaming PU, took foaming kinetics as the core process to control heat generation or heat and mass transfer, and predicted the temperature and density changes of PURF with time when CFC-11 was used as PBA. In the course of research, they noticed the phenomenon of PBA mass loss. However, they did not give an exact mass of losses. Al-Moameri *et al.* [8] used MATLAB to simulate the dynamics and physical characteristics of PURF foaming process, and focused on discussing the mass balance of PBA in the foaming process. However, they directly set the PBA mass loss in the foaming process to 0 in the study without detailed explanations. They quantified

---

✉ Corresponding author: Yingshu Liu E-mail: ysliua@126.com

**Table 1. The relevant properties for each generation of PBA system**

| Generation | PBA | Molecular weight / ($g\cdot mol^{-1}$) | Boiling point / °C | ODP | GWP | Elimination process as PBA |
|---|---|---|---|---|---|---|
| First | CFC-11 | 138 | 24 | 1 | 4000 | It was banned worldwide in 2004. |
| Second | HCFC-141b | 117 | 32 | 0.11 | 630 | It will be banned worldwide in 2030. |
| Third | HFC-245fa | 134 | 15 | 0 | 1030 | None for the time being. |
| Third | HFC-365mfc | 148 | 40 | 0 | 840 | None for the time being. |
| Fourth | HFCO-1233zd(E) | 131 | 19 | 0 | 1 | None for the time being. |
| Fourth | HFO-1336mzzZ | 164 | 33 | 0 | 2 | None for the time being. |

the effectiveness of foaming agent by computer simulation, discussed the mass balance of PBA in the foaming process, and carried out simulation verification, but only controlled the loss of PBA during mixing and stirring in the research process and did not conduct further quantitative research on PBA mass loss in the foaming process.

The final volume of PURF in the physical process of PU box foaming simulated by Shen *et al.* [9] is only 30%–90% of the predicted volume. They believed that a primary mechanism for the inefficiency of PBA is the PBA mass loss through cell rupture (convection) and discussed the relationship between the closed cell ratio of PURF and the PBA mass loss. However, new evidence shows that the mass loss of surface evaporation is the real cause of the PBA mass loss. Details will be discussed in this article.

This work differs in three ways from the other work: (a) taking the bio-based polyol system PURF as the research object, a measurement method of the PBA mass loss, adding water to replace the difference, was designed; (b) different eco-friendly PBA mass losses were measured by this method; (c) the mechanism of PBA mass loss and key influential factors were further clarified. The study of PBA mass loss will provide an effective theoretical basis for the simulation and calculation of several key factors such as density, modulus, and strength of PURF, and will provide ideas and clues for further effectively reducing PBA mass loss rate in PURF foaming process.

## 2. Modeling methods

### 2.1. Method for measuring PBA mass loss

The actual PBA mass loss in PURF foaming process can be calculated by Eqs. (1)–(4):

$$m_1 = (m_b - m_f) - m_p - m_0 \tag{1}$$

$$m_p = \rho_a V_P \tag{2}$$

$$V_P = \frac{m_t - m_a + m_f}{\rho_w} - \frac{m_b}{\rho_m} \tag{3}$$

$$m_0 = m_c a_0 \tag{4}$$

where the actual PBA mass loss $m_l$ (g) in PURF foaming process is the difference between the actual reduced mass ($m_b - m_f$) (g) of foam and the actual mass $m_p$ (g) of air occupied by increased volume during foaming. The PURF was prepared by mixing a polyether blend (A-side) and isocyanate (B-side). A- and B-sides contain a lot of small molecular components. These components in the foaming process will also be released into the air. The actual PBA mass loss $m_l$ in PURF foaming process needs to be ruled out this part of the loss; thus, that is a set of blank group without the PBA experiments. Through this group of experiments, the mass of small molecule loss except PBA in PURF was determined as $m_0$ (g). $a_0$ (wt%) is the ratio of small molecule loss except PBA in PURF. $m_c$ (g) is the material total mass of the foaming start without PBA. The actual increased volume $V_P$ ($cm^3$) of foam was measured by adding water to replace the difference. Moist air density $\rho_a$ ($kg\cdot m^{-3}$) was calculated by a standard formula method. All variables are brought into Eqs. (1)–(4) to calculate the actual PBA mass loss $m_l$ during PURF foaming.

Fig. 1 is a schematic diagram of the method of adding water to replace the difference. Due to the extremely low viscosity and good flowability of water, this method can effectively avoid various defects of foam body in the PURF foaming process, and has a very high fault tolerance rate for foam of different foaming forms. This method can also be used to measure the irregular and solid volume with defects.

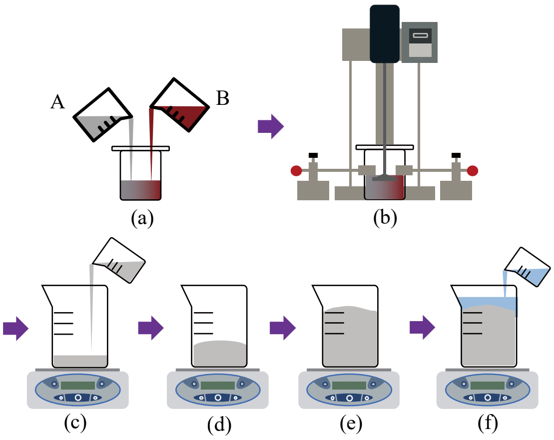

**Fig. 1. The method of adding water to replace the difference: (a) adding A-side and B-side; (b) stirring and mixing; (c) moving into a large beaker for foaming; (d) PURF growth; (e) foam completed; (f) adding water to supplement the vacancy.**

### 2.2. The actual increased volume $V_P$ of foam

Firstly, the standard volume $V_c$ ($cm^3$) of the beaker was set and measured to determine the true volume at the water adding scale. The mass of water added to the scale mark in the empty beaker is $m_t$ (g). After the growth and solidification of foam was completed, the total mass $m_f$ (g) of the system was weighed at the end of foaming. Then the water (watertemperature, $T_w$) was added to the mark, and then the water mass $m_a$ (g) at the scale mark in the beaker was obtained. Finally, the previous variables and the density of PU materials $\rho_m$ ($g\cdot cm^{-3}$) were brought into Eq. (3) to calculate the actual increased volume $V_P$ ($cm^3$) of foam.

### 2.3. Air density measurement and calculation

Many researchers have paid attention to the problem of air buoyancy in the previous work, but they have not considered the influence of air humidity. Since the molecular weights of water vapor and dry air are quite different, the direct calculation of air buoyancy with dry air will have great deviation [6,9].

The density of moist air needs to be measured and calculated. The moist air density estimation methods have been described [10–13]. Generally speaking, there are two basic methods for measuring air density: one is buoyancy method based on Archimedes' law; the other is the formula method, which uses CIPM's recommended formula. Air density measurement by formula method is the most widely used method at present, which is not only easy to implement, but also has a high measurement accuracy. The following is a brief description of CIM-81/91 and CIM-2007 formula.

$$\rho_a = \frac{PM_d}{ZRT}\left[1 - x_v\left(1 - \frac{M_v}{M_d}\right)\right] \tag{5}$$

The density of moist air is evaluated using an equation of state in Eq. (5). Both the new edition and the old edition are employed in this formula, where $P$ (Pa) is the total pressure; $T$ (K) is the moist air temperature; $x_v$ is mole fraction of water vapor; $M_d$ ($kg\cdot mol^{-1}$) is molar mass of dry air; $M_v$ ($kg\cdot mol^{-1}$) is the molar mass of moist air; $Z$ is compressibility factor; $R$ ($J\cdot mol^{-1}\cdot K^{-1}$) is molar gas constant.

Since the measurement and calculation of compressibility factor $Z$ and mole fraction of water vapor $x_v$ are very complicated, the simplified formula is generally used when the accuracy is not very high.

Under normal pressure, moist air can be seen as an ideal mixture of dry air and water vapor, and the small errors caused by compressibility of non-ideal gas are neglected [10], which conforms to the ideal gas state equation. The density of moist air can be written simply as the sum of the density of the contained dry air and water vapor at the temperature of the moist air and the respective independent pressures.

$$\rho_a = \rho_{da} + \rho_v = \frac{P_d}{R_d T} + \frac{P_v}{R_v T} \tag{6}$$

where $\rho_a$ ($kg\cdot m^{-3}$) is the density of moist air; $\rho_{da}$ ($kg\cdot m^{-3}$) is the density of dry air; $\rho_v$ ($kg\cdot m^{-3}$) is the density of water vapor; $P_d$ (Pa) is the pressure due to dry air; $R_d$ = 287.058 $J\cdot mol^{-1}\cdot K^{-1}$, the specific constant of dry air; $P_v$ (Pa) is the pressure due to water vapor; $R_v$ = 461.495 $J\cdot mol^{-1}\cdot K^{-1}$, the specific constant of water vapor [13].

Since $R_d = \frac{R}{M_d}$ and $R_v = \frac{R}{M_v}$, substituting the above formula for further arrangement can be obtained:

$$\rho_a = \frac{P_d M_d + P_v M_v}{RT} \tag{7}$$

where $M_d$ = 0.0289654 $kg\cdot mol^{-1}$, the molar mass of dry air; $M_v$ = 0.018016 $kg\cdot mol^{-1}$, the molar mass of moist air; $R$ = 8.314472 $J\cdot mol^{-1}\cdot K^{-1}$, the gas constant [12].

Among them, $P_d = P - P_v$. Water vapor pressure $P_v$ is calculated based on saturated vapor pressure and relative humidity.

$$P_v = \phi P_s \tag{8}$$

where $\phi$ (wt%) is the relative humidity; $P_s$ (Pa) is the vapor saturation pressure.

In addition, at any given temperature $T_x$, the saturated vapor pressure of water is the vapor pressure at 100wt% relative humidity.

$$\lg P_s = 7.07406 - \frac{1657.46}{T_x + 227.02} \tag{9}$$

The moist air density $\rho_a$ can be conveniently calculated after the total pressure $P$, relative humidity $\phi$, and moist air temperature $T$ obtained from the above formula. Using this method, the error of density calculation is less than 0.2% between 10 and 50°C, which fully meets the overall measurement accuracy of the present experimental method.

## 3. Experimental

### 3.1. Raw materials and experimental apparatus

PM-200: oligomeric isocyanate of 4-4′ diphenyl methane diisocyanate, for which average functionality is 2.7, the percentage of NCO is 31wt%, and viscosity is 180–250 mPa·s at 25°C, industrial grade, Wanhua Chemical Group Co., Ltd.; FH8450: bio-based polyol, for which the hydroxyl number is 420 mg KOH per g, industrial grade, Zhangjiagang Feihang Technology Co., Ltd.; DMCHA and DBTDL: catalysts, industrial grade, Beijing Intech Co., Ltd.; L6900: silicone-type surfactant, industrial grade, Momentive Co.; TCPP: a flame retardant for PURF, industrial grade, Jiangsu Yoke Technology Co., Ltd.; HCFC-141b: blowing agent, Changshu San'aifu Fluorine Chemical Co., Ltd.; HFC-245fa and HFCO-1233zd(E): blowing agents, Honeywell (China), Co., Ltd.; HFC-365mfc: blowing agent, Solvay Co., Ltd; HFO-1336mzzZ: blowing agent, Chemours Chemistry (Shanghai) Co., Ltd.

High speed frequency conversion dispersing machine: JFS1100-ST, Hunan Lichen Instrument Technology Co., Ltd.; Barometer: DYM-3, Shanghai Instrument Technology Co., Ltd.; Hygrograph: GJWS-T1, Shanghai Instrument Technology Co., Ltd.; Electronic balance: JJ2000B, Hangzhou Shuangjie Electronic Computer Co., Ltd.; Ultra-depth 3D microscope: KEYENCE VHX-6000, Japan Ōsaka Co., Ltd.

### 3.2. Experimental procedures

Multiple PBA mass loss rate in the PURF foaming process was measured, and the experimental results were analyzed and studied. Foaming recipes of PURF for group 1 and group 2 are shown in Table 2 and Table 3. Each PBA has been tested at five levels: 10, 20, 30, 40, and 50 g.

At the ambient temperature of 20–25°C, each component of A-side was successively added and mixed evenly accord-

**Table 2. Foaming recipes for group 1 and group 2**

| Side | Ingredient | Function | Weight / g | |
|---|---|---|---|---|
| | | | Group 1 | Group 2 |
| A-side (polyol) | FH8450 | Polyester polyol | 100 | 100 |
| | DMCHA | Catalyst | 1.5 | 1.5 |
| | DBTDL | Catalyst | 0.5 | 0.5 |
| | $H_2O$ | Chemical blowing agent | 1 | 1 |
| | L6900 | Surfactant | 0.5 | 0.5 |
| | TCPP | Fire retardant | 20 | 20 |
| | HCFC-141b | PBA | 25 | — |
| | PBA (see Table 3) | PBA | — | see Table 3 |
| B-side (isocyanate) | PM-200 | Oligomeric isocyanate | 208 | 208 |

**Table 3. PBA loading in the foaming recipes for group 2**

| Ingredient | Weight / g | | | | |
|---|---|---|---|---|---|
| | Level 1 | Level 2 | Level 3 | Level 4 | Level 5 |
| HCFC-141b | 10 | 20 | 30 | 40 | 50 |
| HFC-245fa | 10 | 20 | 30 | 40 | 50 |
| HFC-365mfc | 10 | 20 | 30 | 40 | 50 |
| HFCO-1233zd(E) | 10 | 20 | 30 | 40 | 50 |
| HFO-1336mzzZ | 10 | 20 | 30 | 40 | 50 |

ing to the proportion in Table 1, and the temperature of A- and B-sides was adjusted to (22 ± 0.5)°C. During foaming, appropriate amount of A-side and corresponding proportion of B-side were placed into the same beaker. The mixture was stirred at 2500 r/min for 10 s, and then quickly poured into the plastic beaker used by the method of adding water to replace the difference. During foaming process and after foaming, the corresponding value was recorded and the added water was measured.

## 4. Results and discussion

### 4.1. Reliability verification for the method of adding water to replace the difference

According to the recipes in Table 2, foaming was carried out according to the corresponding experimental steps, and relevant experimental parameters were recorded. The experiments used to determine the mass of small molecule loss except PBA in PURF $m_0$ and to measure the actual PBA mass loss in foaming process $m_1$ were carried out in 7 groups of parallel experiments. The density of water $\rho_w$ used in the experiment is 1.004 $g\cdot cm^{-3}$, the atmospheric pressure (absolute pressure) $P_0$ is 99.95 kPa, and the mass of water added to the scale mark in the empty beaker $m_t$ is 994.13 g. According to the basic data measured and Eqs. (1)–(9), the ratio of small molecule loss except PBA in PURF $a_0$ can be calculated, as shown in Table 4.

**Table 4. The basic mass loss rate ($a_0$) without PBA**

| Statistical indicator | PBA weight / g | $\omega$ / wt% | $a_0$ / wt% |
|---|---|---|---|
| Average | 0 | 0 | 0.130 |
| $\sigma$ | — | — | 0.005 |

Note: $\sigma$—Standard deviation.

In Table 4, $\omega$ is the PBA mass accounted for the total amount of materials (sum of A- and B-side) except the PBA in PURF, that is, the initial mass content of PBA in PU materials.

$$\omega = \frac{m_2}{m_b - m_2} \times 100\% \tag{10}$$

where $m_2$ (g) is the PBA mass in the material total mass.

The ratio of small molecule loss except PBA in PURF $a_0$ takes its average value of 0.130wt% as the intermediate variable of subsequent calculation. By combining the basic data measured, the basic mass loss rate without PBA $a_0$, and Eqs. (1)–(9), the PBA mass loss ratio in PURF foaming process can be calculated, as shown in Table 5.

**Table 5. The PBA mass loss ratio in PURF foaming process with the recipes group 1 in Table 2**

| Statistical indicator | HCFC-141b weight / g | $\omega$ / wt% | $R_1$ / wt% | $R_2$ / wt% |
|---|---|---|---|---|
| Average | 25 | 7.01 | 0.65 | 7.47 |
| $\sigma$ | — | — | 0.028 | 0.406 |

In Table 5, $R_1$ is ratio of the PBA mass loss to the material total mass except the PBA in PURF foaming process, $R_2$ is ratio of the PBA mass loss to the PBA mass in the material total mass of PURF foaming process.

$$R_1 = \frac{m_1}{m_b - m_2} \times 100\% \tag{11}$$

$$R_2 = \frac{m_1}{m_2} \times 100\% \tag{12}$$

In the same foaming recipes, the data dispersion degree of $R_1$ and $R_2$ can effectively reflect the reliability of the test method, the quantitative values can be expressed by standard deviation $\sigma$, Fig. 2 and Fig. 3 respectively show the discreteness of $R_1$ and $R_2$ in the parallel experimental groups.

As can be seen from Table 5, Fig. 2, and Fig. 3, the repeatability of $R_1$ and $R_2$ in the parallel experimental groups is good. The standard deviations are 0.028wt% and 0.406wt% respectively, and the ratio of standard deviation to average is 4.35% and 5.44% respectively, indicating that the experimental scheme used in this study is stable and reliable with good repeatability. It can be used to calculate and study the actual PBA mass loss in PURF foaming process.

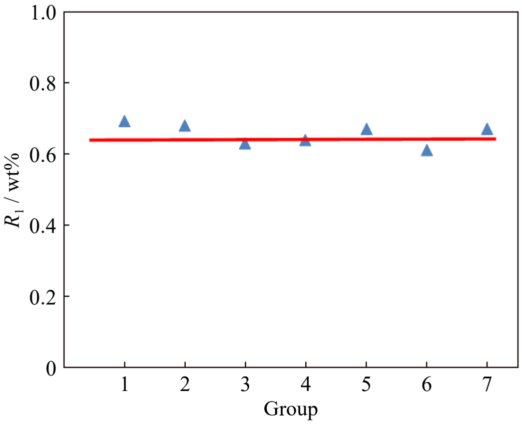

**Fig. 2. $R_1$ in the PURF foaming process with HCFC-141b system for parallel experimental groups. The red line represents the average.**

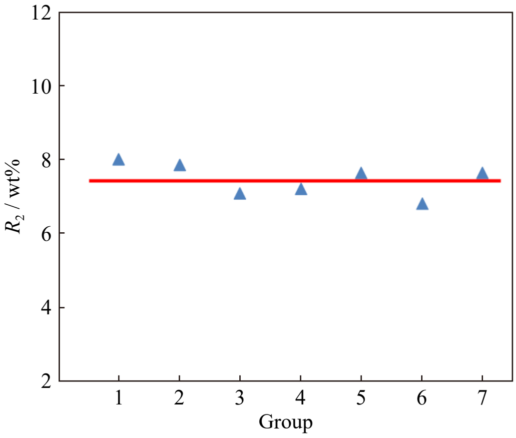

**Fig. 3. $R_2$ in the PURF foaming process with HCFC-141b system for parallel experimental groups. The red line represents the average.**

### 4.2. Actual PBA mass loss in foaming process of bio-based PURF with various PBA systems

The actual PBA mass loss rate of the second, third, and fourth generation PBA in the bio-based PURF was measured by adding water to replace the difference. The third and fourth generation PBA are eco-friendly PBA, which have 0 ODP.

Recipes group 2 in Table 2 were used to perform foaming operations according to corresponding experimental procedures, and relevant experimental parameters were recorded. The density of water $\rho_w$ used in the experiment is 1.004 g·cm$^{-3}$, and the mass of water added to the scale mark in the empty beaker $m_t$ is 994.13 g. The average value of $a_0$ in Table 4 is 0.130wt%, which is used as the basic mass loss rate without PBA. The ratios of PBA mass loss $R_1$ in different PURF foaming processes can be calculated by combining Eqs. (1)–(9). In each group of different PBA foaming systems, the effects of six different PBA initial mass contents $\omega$ on the actual PBA mass loss during the foaming process were tested respectively. The average values of the final $R_1$ of all test groups are summarized in Table 6.

**Table 6. Different PBA mass loss rates $R_1$ for the test groups**

| $\omega$ / wt% | $R_1$ / wt% | | | | |
|---|---|---|---|---|---|
| | HCFC-141b | HFC-245fa | HFC-365mfc | HFCO-1233zd(E) | HFO-1336mzzZ |
| 0 | 0.00 | 0.00 | 0.00 | 0.00 | 0.00 |
| 3.02 | 0.25 | 0.19 | 0.15 | 0.20 | 0.14 |
| 6.03 | 0.45 | 0.37 | 0.32 | 0.44 | 0.26 |
| 9.05 | 0.68 | 0.72 | 0.52 | 0.65 | 0.46 |
| 12.06 | 1.03 | 0.94 | 0.70 | 0.93 | 0.66 |
| 15.08 | 1.31 | 1.14 | 0.97 | 1.19 | 0.78 |

$R_1$ is not only an important index to measure the reliability and repeatability of the experimental scheme, but also an important index of the escape behavior of PBA in the foaming process. The higher the values of $R_1$, the higher the loss rate of PBA in the foaming process, and the more attention should be paid to the environmental protection, safety, and economic benefits.

Fig. 4 shows the relationship of $R_1$ and the initial mass content of PBA, $\omega$, in PU materials. PURF foams with different PBAs are indicated by different symbols. The data are obtained from Table 6.

$R_1$ with different PBA systems showed a approximately linear change with $\omega$, and its linear correlation index "$R^2$" reached above 0.988. The results show that the PBA mass loss in PURF with different PBA systems is controlled by its initial mass content of PBA in PU materials $\omega$. There is a significant difference between $R_1$ for different PBAs. With the

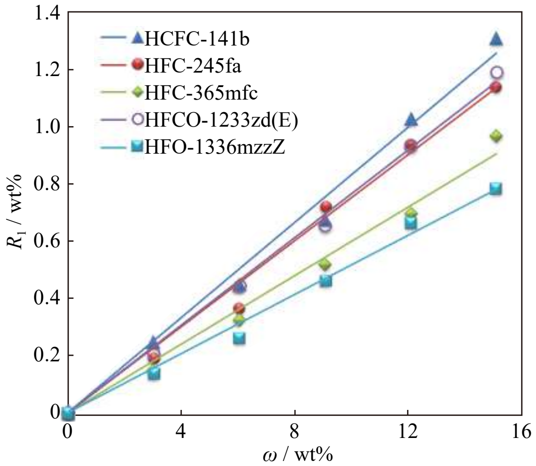

**Fig. 4. Relationship of $R_1$ and the initial mass content of PBA, $\omega$, in PU materials.**

fixed $\omega$ value, the $R_1$ values of PURF foams using different PBAs can demonstrate their escape capacities during the foaming process. The higher the $R_1$ value, the higher the escape capacity.

### 4.3. The PBA mass loss mechanism

Possible sources for weight loss are (1) air's buoyant force applied by the increasing volume of the foam, (2) rupture of foam cells (bubbles) with collapse of the cell or replacement of the vapors by new vapors, and (3) evaporation/escape of PBA, water, or carbon dioxide along the upper surface of the foam [9].

The air buoyancy exerted by the increase of foam volume has been explained and calculated in this study, and the remaining two possible reasons need to be further analyzed and determined in combination with the results of this study. Shen *et al.* [9] believed that a primary mechanism for the inefficiency of PBA is the PBA mass loss through cell rupture (convection). This process requires two conditions: (1) a lot of open cells in the foam at the initial stage of foaming; (2) the internal opening cells are communicated with the foam surface, and PBA is continuously dissipated into the air through surface opening or bubble breaking in the foaming process. During the foaming process, the internal cell state can't be actually observed, but the foam surface state can be actually observed and finally whether there is a continuous gas path can be confirmed by microscopic observation.

Fig. 5 shows the continuous change process of the upper surface of the PU foam during the foaming process. Obviously, during the whole foaming process, the upper surface of the foam is continuous and complete, and even a large number of air bubbles brought in during the stirring process are not damaged before the foam solidifies. Fig. 6 shows the ultra-depth 3D micrographs of the foam surface state at different magnifications, and it can be clearly seen that the foam surface is composed of non-foamed skin with discontinuous small bubbles. Under the condition of coaxial illumination, the surface of thin layer foam becomes transparent, the surface reflection of different small bubbles and the surface wrinkles of individual bubbles are clearly visible, all bubbles are not damaged, and the non-foamed parts are compact and complete. It can be confirmed that there is no path for PBA to dissipate into the air through surface holes or bubbles.

Obviously, evaporation/escape along the upper surface of foam is the main way for PBA mass loss to the air. The previous experimental data also confirm this result well.

Microscopically, polyurethane foam can be regarded as a liquid with very low viscosity before gelation [7], and PBA continuously migrates from high concentration to low concentration by dissolving in foam continuous phase. At the interface layer between foam and air, the ambient air is constantly flowing, and the PBA concentration in the air can be

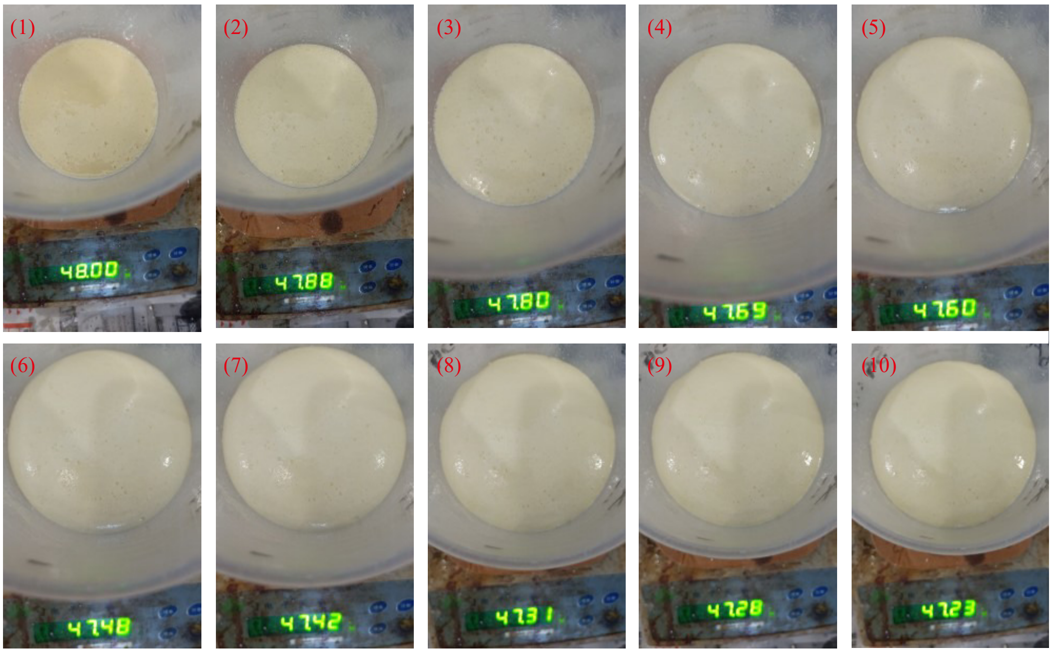

**Fig. 5.  Continuous change process of the upper surface of the foams: (1)–(10) are the corresponding figures of PURF upper surface changing with the foaming time increase, and the green number shows the material total mass during foaming.**

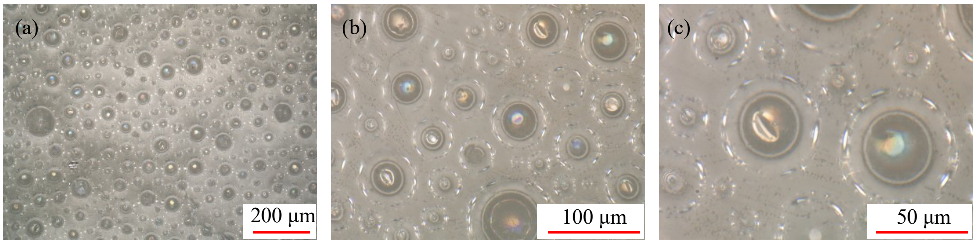

**Fig. 6.  PURF with HCFC-141b system foam surface state at different magnifications: (a) 300 times, (b)1000 times, and (c) 2000 times.**

neglected. The chemical potential of PBA in the interface layer is much higher than that in the outside air, which leads to the diffusion potential difference. Therefore, the evaporation/escape of PBA along the upper surface of foam is a typical diffusion behavior.

Fick's first diffusion equation (Eq. (13)) shows that the molar flux caused by diffusion is proportional to the concentration gradient. Obviously, in the interface layer between foam and air, the concentration gradient $\nabla c$ (mol·cm$^{-4}$) can be considered as the difference between PBA concentration in interface layer and PBA concentration in air. $\nabla c$ is equal to PBA concentration in interface layer when ignoring PBA concentration in air.

$$N = -D\nabla c \tag{13}$$

where $N$ (mol·cm$^{-2}$·s$^{-1}$) is diffusion flux; $D$ (m$^2$·s$^{-1}$) is diffusion coefficient.

Furthermore, the PBA concentration in the interface layer is positively correlated with the PBA content contained in the foam. The PBA mass loss in the PURF foaming process is actually the integral value of PBA molar flux per unit time on the foam surface within a period of time from foam initiation to gel curing under the constraint of Fick's diffusion equation. From the experimental results, it can be seen that $R_1$ with different PBA foaming systems has an approximately linear change with $\omega$ (Fig. 4). Therefore, it can be further confirmed that the PBA dissolved in the foam in the foaming process also changes approximately linearly. As different PBA have different property, the change rates of their respective dissolved amount are different and the diffusion coefficients in the interface layer are also different in different PBA systems, which leads to different slopes of $R_1$ with the change of $\omega$ in different PBA systems.

From the above analysis, it can be inferred that PBA with similar attributes will have similar diffusion behavior, and then have similar PBA mass loss behavior during the foaming process. The $R_1$ values vs. $\omega$ for HFC-245fa and HFCO-1233zd(E) almost coincide (Fig. 4), which shows that HFC-245fa and HFCO-1233zd(E) are close in physical and chemical characteristics, and that is actually true. Table 1 shows the data of molecular weight and boiling point of six PBAs. Obviously, the molecular weight and boiling point of HFC-245fa and HFCO-1233zd(E) are the closest.

This research is based on the bio-based PURF, but it can be seen from the above results that this research conclusion can be extended to the petroleum-based PURF, because the core chemical reaction processes of the two are similar. The results show that for a certain foaming system, $R_1$ has a linear relationship with $\omega$, which can be expressed by the functional relationship (Eq. (14)).

$$R_1 = k\omega \tag{14}$$

where $k$ is a variable related to PBA's own attributes, and the solution of $k$ will be the next key research work.

## 5. Conclusions

Through systematical experiment design, multiple eco-friendly PBA mass loss of bio-based PURF in the foaming process was measured and calculated in this study. The foam volume was determined and measured by adding water after the foam solidified. The wet air density was calculated by the moist air density standard formula, and then the real mass change of foam was measured by air buoyancy removal method and PBA-free base mass loss rate calibration method. The combination of the two methods can accurately measure and calculate the PBA mass loss. Since water has very low viscosity and good flowability, this method can effectively avoid various defects of foam in the foaming process, and has a high fault tolerance rate for different foaming forms of foam.

Using this method, different eco-friendly PBA mass losses were measured quantitatively for the first time. The method was proved to be stable and reliable through the standard deviations $\sigma_1$ and $\sigma_2$ for $R_1$ (ratio of the PBA mass loss to the material total mass except the PBA) and $R_2$ (ratio of the PBA mass loss to the PBA mass in the material total mass) in parallel experiments. The $\sigma_1$ and $\sigma_2$ are 0.028wt% and 0.406wt%, respectively, and the ratio of $\sigma_1$ and $\sigma_2$ to average is 4.35% and 5.44%, respectively. It can be used to measure and calculate the actual PBA mass loss in the foaming process of both bio-based and petroleum-based PURF. The results show that the PBA mass loss in PURF with different PBA systems is controlled by its initial mass content of PBA in PU materials $\omega$. There is a significant difference between $R_1$ for different PBAs. With the fixed $\omega$ value, the $R_1$ value of PURF foams using different PBA can demonstrate their escape capacity during the foaming process. The higher the R1 value, the higher the escape capacity.

This study confirms that evaporation/escape along the upper surface of foam is the main way for PBA mass loss to the air. The PBA mass loss mechanism is as follows: the evaporation/escape of PBA along the upper surface of foam is a typical diffusion behavior. Its spread power comes from the difference between the chemical potential of PBA in the interface layer and that in the outside air. PBA with similar attributes will have similar diffusion behavior, and then have similar PBA mass loss behavior during PURF foaming process.

For a certain PURF system, $R_1$ has approximately linear relationship with the initial mass content of PBA in PU materials $\omega$, which can be expressed by the functional relationship $R_1 = k\omega$, where $k$ is a variable related to PBA's own attributes.

## Conflict of Interest

The authors declare no potential conflict of interest.

## Nomenclature

| | |
|---|---|
| $a_0$ | The ratio of small molecule loss except PBA in PURF, wt% |
| $D$ | Diffusion coefficient, m$^2$·s$^{-1}$ |
| $k$ | A variable related to PBA's own characteristics |

| | |
|---|---|
| $m_0$ | The mass of small molecule loss except PBA in PURF, g |
| $m_1$ | The actual PBA mass loss, g |
| $m_2$ | The PBA mass in the material total mass, g |
| $m_a$ | The mass of adding water to the scale mark in the beaker after completion of foaming, g |
| $m_b$ | Material total mass for the foaming start, g |
| $m_c$ | Material total mass of the foaming start without PBA, g |
| $m_f$ | Material total mass for the foaming end, g |
| $m_p$ | The actual mass of air occupied by increased volume during foaming, g |
| $m_t$ | The mass of water added to the scale mark in the empty beaker, g |
| $M_d$ | The molar mass of dry air, $kg\cdot mol^{-1}$ |
| $M_v$ | The molar mass of moist air, $kg\cdot mol^{-1}$ |
| $N$ | Diffusion flux, $mol\cdot cm^{-2}\cdot s^{-1}$ |
| $P$ | Total pressure, Pa |
| $P_0$ | Atmospheric pressure, kPa |
| $P_d$ | Pressure due to dry air, Pa |
| $P_s$ | The vapor saturation pressure, Pa |
| $P_v$ | Pressure due to water vapor, Pa |
| $R_1$ | Ratio of the PBA mass loss to the material total mass except the PBA in PURF foaming process, wt% |
| $R_2$ | Ratio of the PBA mass loss to the PBA mass in the material total mass in PURF foaming process, wt% |
| $R$ | Molar gas constant, $J\cdot mol^{-1}\cdot K^{-1}$ |
| $R_d$ | The specific constant of dry air, $J\cdot mol^{-1}\cdot K^{-1}$ |
| $R_v$ | The specific constant of water vapor, $J\cdot mol^{-1}\cdot K^{-1}$ |
| $T$ | Moist air temperature, K |
| $T_w$ | Water temperature, K |
| $T_x$ | Given temperature, °C |
| $V_P$ | The volume of foam actually increased, $cm^3$ |
| $V_c$ | The volume of the beaker below the mark, $cm^3$ |
| $x_v$ | Mole fraction of water vapor |
| $Z$ | Compressibility factor |
| $\rho_m$ | The density of polyurethane material after mixing, $g\cdot cm^{-3}$ |
| $\rho_a$ | The density of (moist) air, $kg\cdot m^{-3}$ |
| $\rho_w$ | The density of water, $g\cdot cm^{-3}$ |
| $\rho_{da}$ | The density of dry air, $kg\cdot m^{-3}$ |
| $\rho_v$ | The density of water vapor, $kg\cdot m^{-3}$ |
| $\phi$ | The relative humidity, wt% |
| $\omega$ | The initial mass content of PBA in PU materials, wt% |
| $\nabla c$ | Concentration gradient, $mol\cdot cm^{-4}$ |
| $\sigma$ | Standard deviation |

## References

[1] M.F. Sonnenschein, *Polyurethanes: Science, Technology, Markets, and Trends*, John Wiley & Sons, Inc., Hoboken, 2014.

[2] J.M. Kim, D.H. Kim, J. Kim, J.W. Lee, and W.N. Kim, Effect of graphene on the sound damping properties of flexible polyurethane foams, *Macromol. Res.*, 25(2017), No. 2, p. 190.

[3] G. Coste, C. Negrell, and S. Caillol, From gas release to foam synthesis, the second breath of blowing agents, *Eur. Polym. J.*, 140(2020), art. No. 110029.

[4] J. Wu, A. Albouy, and D. Mouton, Evaluation of the next generation HFC blowing agents in rigid polyurethane foams, *J. Cell. Plast.*, 35(1999), No. 5, p. 421.

[5] S.K. Wang, Z.K. Guo, X.H. Han, X.G. Xu, Q. Wang, S.M. Deng, and G.M. Chen, Experimental evaluation on low global warming potential HFO-1336mzz-Z as an alternative to HCFC-123 and HFC-245fa, *J. Therm. Sci. Eng. Appl.*, 11(2019), No. 3, art. No. 031009.

[6] S.A. Baser and D.V. Khakhar, Modeling of the dynamics of R-11 blown polyurethane foam formation, *Polym. Eng. Sci.*, 34(1994), No. 8, p. 632.

[7] S.A. Baser and D.V. Khakhar, Modeling of the dynamics of water and R-11 blown polyurethane foam formation, *Polym. Eng. Sci.*, 34(1994), No. 8, p. 642.

[8] H.H. Al-Moameri, G. Hassan, and B. Jaber, Simulation physical and chemical blowing agents for polyurethane foam production, *IOP Conf. Ser.: Mater. Sci. Eng.*, 518(2019), No. 6, art. No. 062001.

[9] L. Shen, Y.S. Zhao, A. Tekeei, F.H. Hsieh, and G.J. Suppes, Density modeling of polyurethane box foam, *Polym. Eng. Sci.*, 54(2014), No. 7, p. 1503.

[10] A. Picard, R.S. Davis, M. Gläser, and K. Fujii, Revised formula for the density of moist air (CIPM-2007), *Metrologia*, 45(2008), No. 2, p. 149.

[11] R.S. Davis, Equation for the determination of the density of moist air (1981/91), *Metrologia*, 29(1992), No. 1, p. 67.

[12] P. Giacomo, Equation for the determination of the density of moist air (1981), *Metrologia*, 18(1982), No. 1, p. 33.

[13] G.R. North, J. Pyle, and F.Q. Zhang, *Encyclopedia of Atmospheric Sciences*, 2nd ed., Elsevier, London, 2015.